Biochimica et Biophysica Acta 812 (1985) 643–655
Elsevier

BBA 72416

The shape of lipid molecules and monolayer membrane fusion

L.V. Chernomordik, M.M. Kozlov, G.B. Melikyan, I.G. Abidor, V.S. Markin and Yu.A. Chizmadzhev

A.N. Frumkin Institute of Electrochemistry, Academy of Sciences of the USSR, Leninsky Prospect 31, Moscow 117071 (U.S.S.R.)

(Received April 18th, 1984)
(Revised manuscript received September 27th, 1984)

Key words: Membrane fusion; Lipid shape; Trilaminar structure; Electrical breakdown

The contact between two bilayer membranes results in their monolayer fusion comprising the formation of a trilaminar structure (a single bilayer connected to two bilayers over the whole perimeter) in the contact region. The time required for monolayer fusion was measured and irreversible electrical breakdown was studied for membranes of different compositions. A theoretical model of the monolayer fusion is suggested to explain the results. It assumes that the structural reorganization underlying the process involves the formation of a stalk between bilayers as a result of local bending of the interacting monolayers. This structural reorganization is similar to the hydrophilic pore formation in a bilayer under irreversible breakdown. However, the directions of the monolayer bending are different in the two processes and, therefore, the bending energies depend oppositely on the effective shape of lipid molecules. Theoretical predictions agree well with experimental data. The applicability of the suggested mechanism to biomembrane fusion is discussed.

Introduction

In recent years, a number of papers have appeared dealing with the mechanism of cellular membrane fusion and prefusion membrane interaction (for a review, see Ref. 1). The fusion can be conveniently subdivided into the following stages [2]: First, a tight hydrophobic contact occurs between the protein-free membrane regions [2,3]. The subsequent stages of the process have not been established with any certainty, different viewpoints being based mainly on the results of electron-microscopy investigations. De Kruijff et al. [4] proposed that the fusion is a result of nonbilayer structure formation (of the type of inverted micelles) in the contact region. There is evidence, however, that membrane fusion is preceded by the formation of an intermediate (so-called trilaminar) structure in the contact region [2,5,6], when two bilayers interact to yield a single bilayer. Further disruption of this bilayer leads to joining of the interiors of the cells or vesicles, i.e., to their fusion.

Membrane fusion cannot proceed without disturbing the lipid bilayers. It requires a drastic structural reorganization of the membranes involving the development of structural defects. The primary act of a fusion (comprising the beginning of the structural reorganization) determines the mechanism of the process. Two main types of fusion mechanism [7] are worth mentioning: The first one involves, as the primary stage, local structural reorganization of interacting membranes

Abbreviations: PC, phosphatidylcholine; lysoPC, lysophosphatidylcholine; PE, phosphatidylethanolamine.

followed by the formation of a stalk between two bilayers [7,8].

The stalk may consist of either one or two monolayers from a bilayer. Monolayer stalks yield trilaminar structures, whereas bilayer stalks result immediately in complete fusion [8]. The stalks also seem to be observed in multilayer systems, including cardiolipin [6,9]. Secondly, the structural reorganization of membranes involves, simultaneously, wide areas of membrane surfaces. This requires tight adhesion of the bilayers and the second mechanism is, therefore, called the 'adhesion' mechanism [7].

A system of two interacting bilayer lipid membranes provides a convenient experimental model for studying fusion mechanisms [10–16]. The membranes are initially brought together by pressing one membrane against the other until plane-parallel contact is reached between them. After some time, depending on the membrane composition, as well as on the composition and concentration of the electrolyte, the system undergoes the transition to a new state. Simple electrical measurements (usually specific capacity measurements) proved that a single bilayer, i.e., trilaminar structure, was formed in the contact region. Then, provided certain conditions exist, such a monolayer fusion (i.e., the removal of the inner membrane monolayers leading to a contact of the outer monolayers [11,14,16]) may result in complete fusion, with formation of a membrane tube [15]. Thus, the studies of both electrostimulated [15] and Ca^{2+}-induced [16] membrane fusion demonstrated that complete fusion was necessarily preceded by formation of a trilaminar structure in the contact region.

The present work is devoted to theoretical and experimental studies of the mechanism of monolayer membrane fusion. Particular attention is paid to the role of the effective shape of lipid molecules in this phenomenon [17]. It should be noted that the influence of the shape of lipid molecules on structural reorganization of bilayers was already discussed in a number of works [17–25]. It was particularly shown that such asymmetric lipids as phosphatidylethanolamine and cardiolipin can provoke the formation of nonbilayer structures of the type of the inverted hexagonal H_{II} phase [22,23], as well as the occurrence of intramembrane particles within the fusing membranes [24]. It was also reported [25] that bilayer structures can be formed from a mixture of two shape-complementary lipids (e.g., nonsaturated phosphatidylethanolamine and lysophosphatidylcholine), although the individual lipids could not produce planar bilayers.

It is shown in the present work that structural reorganization of bilayer lipid membranes, underlying the monolayer fusion, consists of the formation of a stalk between the bilayers as a result of local bending of the interacting monolayers. In principle, this process is opposite to hydrophilic pore formation in a bilayer under irreversible breakdown [26,27]; the directions of the monolayer bending are different in these processes and, therefore, the bending energies depend oppositely on the spontaneous curvature of lipids in a membrane reflecting the shape of lipid molecules. This close analogy is used below for a comparative study of monolayer fusion and irreversible breakdown of lipid membranes of various compositions.

Theory

Consider the stalk mechanism of membrane fusion involving the formation of a stalk between contacting monolayers of two opposing membranes (Fig. 1). Bulging defects develop initially in the interacting membranes, growing then towards each other. These defects are the nuclei of a stalk and comprise disruptions of the monolayers. Therefore,the energy of the contact between a disruption region and an intermembrane milieu is characteristic of them. This energy per unit nucleus will be denoted as W_r. Further mutual joining of the bulging defects results in the formation of a

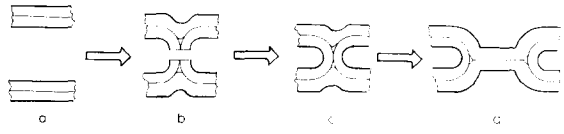

Fig. 1. Stalk mechanism of trilaminar structure formation: (a) two bilayers in contact region; (b) rise of the bulging defects in the contacting monolayers; (c) joining of the defect leading to a stalk formation; (d) removal of the inner monolayers from the contact region and further joining of the outer monolayers resulting in a trilaminar structure formation.

stalk (Fig. 1b, c, d) which is then able to expand. Consider the criteria of the formation and evolution of a stalk. The stalk membrane is bent significantly and possesses, therefore, a considerable bending energy. The monolayer bending energy per unit area [17] is:

$$W = \frac{D_b}{2}(K_1 + K_2 - 2K_s)^2 \quad (1)$$

where K_1 and K_2 are the principal curvatures of a neutral monolayer surface, not changing its area under bending; D_b is the monolayer bending modulus; K_s is the spontaneous curvature representing a monolayer curvature in a stain-less state. Spontaneous curvature of a monolayer comprises a characteristic of the effective shape of the lipid molecules constituting it. The shape of a lipid molecule is determined by the relative size of its polar head and hydrophobic tail [21]. Thus, the packing parameter $f = v(a \cdot l_c)^{-1}$ is used to characterize the shape of a molecule [27] (v is the volume of a molecule, a is the area of its polar head and l_c is the maximal length of its hydrocarbon tail). If $f < 1/3$ (lysolipids), then a molecule has the shape of a cone (Fig. 2a); if $f \approx 1$, a molecule is cylindrically shaped (phosphatidylcholine); and if $f > 1$, a molecule represents an inverted cone (phosphatidylethanolamine). Consider a monolayer composed of lipid molecules of the same kind. In a strain-less state, it possesses a curvature ζ_s referred to as spontaneous curvature of molecules of this type. The spontaneous curvature of a lipid molecule is related to its packing parameter f by $3f(1 + 1/2\zeta_s l_c)^2 = 3 + 1/4 \cdot (\zeta_s l_c)^2$. This relation can be obtained by substituting the explicit expressions for the volume of a molecule and the area of its head into the expression for f. For conical lipids ($f < 1$) the spontaneous curvature is positive, for cylindrical lipids ($f \approx 1$) it equals zero, and for lipids with the shape of an inverted cone ($f > 1$) the curvature is negative (Fig. 2). For a monolayer composed of a mixture of lipid molecules of different kinds, its spontaneous curvature K_s will be related to the respective characteristics of the constituting molecules.

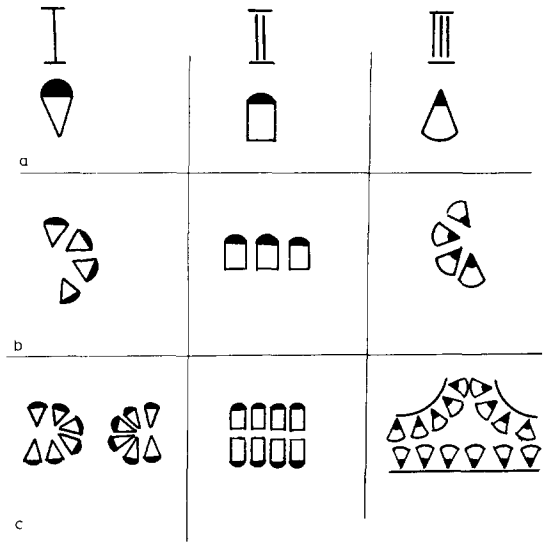

Fig. 2. The shapes of lipid molecules (a), energetically favorable structures formed in a monolayer by lipids of different shapes (b), and typical defects in a bilayer membrane (c). (Ia) A lipid with the polar head exceeding in cross-section the hydrophobic tail – cone (e.g., lysoPC). (Ib) A monolayer of positive spontaneous curvature. (Ic) A hydrophilic pore in a bilayer. (IIa) Cylindrically-shaped lipid (e.g., PC). (IIb) Planar monolayer. (IIc) Defect-less bilayer structure. (IIIa) Inverted cone (e.g., PE). (IIIb) A monolayer of negative spontaneous curvature. (IIIc) Local bulging defect.

It is obvious that the spontaneous curvature of a monolayer can be varied either discretely or continuously. Monolayers of a uniform composition evidently allow us to obtain only a discrete set of K_s values. In the present work, we varied the spontaneous curvature continuously by changing the relative content of lipid components with spontaneous curvatures ζ_{s1} and ζ_{s2}. If it is accepted that the spontaneous curvature of a composite monolayer is additive in spontaneous curvatures of the constituting molecules, then

$$K_s = \theta\zeta_{s1} + (1-\theta)\zeta_{s2} = \zeta_{s2} + (\zeta_{s1} - \zeta_{s2})\theta \quad (2)$$

where θ is the mole fraction of molecules of the first kind.

Spontaneous curvature corresponds to a non-strained shape of the membrane monolayer. Therefore, if the sum of the geometrical curvatures of a monolayer is equal to its doubled spontaneous curvature, then, according to Eqn. 1, the bending energy equals zero. If the sum differs from $2K_s$, then elastic strains occur in the membrane and the respective bending energy (cf. Eqn. 1) becomes not equal to zero. Thus, the bending energy of a

membrane monolayers is lower as the difference between the sum of the geometrical curvatures and the doubled spontaneous curvature becomes smaller. With this in mind, consider the stalk energy. As seen from Fig. 1, a stalk membrane is characterized by two principal curvatures of opposite sign: negative meridianal curvature K_1 corresponding to the stalk generatrix, and positive equatorial curvature K_2 corresponding to a perpendicular direction. Consideration of the stalk geometry revealed that the sum of the curvatures $K_1 + K_2$ is negative because the main term is K_1. Therefore, the stalk formation is the more energetically favourable as the spontaneous curvature of a monolayer is decreased.

Elastic energy can exist even in a planar monolayer due to the non-zero value of its spontaneous curvature. A comparison of the energies of a stalk and planar monolayer determines the possibility of the rise and further evolution of a stalk.

Eqn. 3 gives an expression for the stalk energy with respect to the energy of a planar monolayer as a zero reference point [18]:

$$W_s = 2\pi D_b \left\{ K_s h[\pi(\rho+2)-4] + 2\frac{(\rho+2)^2}{\sqrt{(\rho+2)^2-1}} \arctan\sqrt{\frac{\rho+3}{\rho+1}} - 4 \right\} \quad (3)$$

where $\rho = 2R/h$; h is the thickness of a monolayer, and R is the stalk radius. The analysis of Eqn. 3 shows that the stalk energy should indeed decrease with the decrease of the spontaneous curvature. Suppose that one of the lipid components of a membrane possesses a positive spontaneous curvature, $\zeta_{s1} > 0$, whereas the second component is characterized by a negative curvature, $\zeta_{s2} < 0$, then, in accordance with Eqn. 2, stalk energy (Eqn. 3) will increase with the increase of the content of the first component, since the spontaneous curvature of a membrane monolayer will increase in this case.

A stalk arises as two membranes approach each other. Let us estimate the mean waiting time passing from the instant of apposing membranes together to the instant of a stalk formation. Suppose that an intermediate structure develops initially, composed of two nuclei of zero radius. Its energy is:

$$W_b = 2W_r + W_s$$

and represents the energy barrier which interacting membranes overcome due to fluctuations. Denoting the mean frequency of membrane fluctuations as μ_0; then, the mean waiting time of a stalk formation is:

$$t_{mf} = \mu_0^{-1} \exp\left\{ \frac{1}{kT}(2W_r + W_s) \right\} \quad (4)$$

Statement of the problem

Suppose that the first component (the lipid molecules with positive spontaneous curvature ζ_{s1}), is present in the surrounding solution, its bulk concentration being c_0. If the distribution coefficient of this lipid between a membrane and solution is A, its fraction in a membrane is $\theta = A \cdot c_0$. Let us find the dependence of the waiting time of a stalk formation on the bulk concentration of the first lipid component. Substituting Eqns. 2 and 3 into Eqn. 4, we get:

$$\log t_{mf} = B + 6.15\frac{D_b}{kT} h(\zeta_{s1} - \zeta_{s2}) A c_0 \quad (5)$$

where B embodies all terms independent of the bulk concentration c_0 of the first component. Eqn. 5 shows that if the formation of a trilaminar structure follows the stalk mechanism, the logarithm of the waiting time is proportional to the bulk concentration c_0 of the first component which, when included into a membrane, increases the spontaneous curvature of membrane monolayers. The waiting time increases with c_0, since the stalk energy increases with the spontaneous curvature.

Both $\log t_{mf}$ and c_0 can be experimentally determined, and if the stalk mechanism of a monolayer fusion is realized in a system, a linear dependence of $\log t_{mf}$ on c_0 should be anticipated. This allows us to suggest an independent method of testing the hypothesis that it is the bending strains associated with a spontaneous curvature that cause monolayer fusion. It is based on the fact that the spontaneous curvature of a membrane monolayer

may affect, along with the stalk formation, another structural reorganization of a lipid bilayer, namely the formation of a hydrophilic pore with the edge covered with the heads of lipid molecules (Fig. 2c). The monolayer is bent at the edge of a pore and, therefore, possesses an elastic energy. Notice that the monolayer bending at the edge of a pore is quite similar to the bending of a stalk membrane (Fig. 2). The only difference is the signs of curvatures, i.e., monolayers are bent oppositely in these cases. From this, it follows that the energy of a monolayer bending at the edge of a pore is proportional to the spontaneous curvature K_s but decreases with it, unlike the case of a stalk where the energy increases. The dependence of the energy of a pore edge (per unit length) on the bulk concentration of the first component is:

$$\gamma = \frac{\pi D_b}{h} - \frac{2\pi D_b}{h}\zeta_{s2}h - \frac{2\pi D_b}{h}(\zeta_{s1} - \zeta_{s2})hAc_0 \qquad (6)$$

As seen from Eqn. 6, the edge energy, like the stalk energy, is proportional to the bulk concentration c_0 of the first component, but decreases with it. Compare Eqns. 5 and 6. It is important that the same combination of parameters $\xi = Ah(\zeta_{s1} - \zeta_{s2})D_b$ enters both equations. This fact can be used to test the hypothesis of stalk mechanism, since the edge energy of a pore can be determined from the data on irreversible breakdown of a bilayer [26].

It was found that an electrical field applied to a bilayer stimulates the development of hydrophilic pores in a membrane. The increase of the radius of these pores above a certain critical value leads to irreversible rupture of a membrane. The mean lifetime t_l of a bilayer in an electric field is described by the following expression [26]:

$$t_l = P \cdot \exp\left\{\frac{\pi\gamma^2}{kT\left[\sigma + C_m(\epsilon_s/\epsilon_m - 1)V^2/2\right]}\right\} \qquad (7)$$

Here, P is the preexponential factor, k the Boltzmann constant, T the absolute temperature, σ the tension, C_m the capacity of a membrane, $\epsilon_s = 80$ and $\epsilon_m = 2$ and are the permeabilities of the surrounding solution and the hydrocarbon part of a membrane, respectively, and U the voltage applied to a membrane. Knowing the experimental dependence of t_l on U, Eqn. 7 allows evaluation of the value of γ determined also by Eqn. 6. Knowing the experimental dependence of γ on c_0 and Eqn. 6, one can find parameter ξ. Substituting this parameter into Eqn. 5, one obtains the theoretical dependence of $\log t_{mf}$ on c_0. Its comparison with the corresponding experimental results can be used to verify the hypothesis that the structural reorganization leading to a trilaminar structure formation is a result of bending strains and is determined by the spontaneous curvature of a bilayer.

Experimental

Materials. Lipid bilayers were prepared from phosphatidylethanolamine (PE, ex *Escherichia coli*, Koch-Light), azolectin (Associated Concentrates), cardiolipin ex bovine heart (Kharkov, U.S.S.R.), egg phosphatidylcholine (PC, Koch-Light) and general lipids of bovine brains obtained by the method described by Kates [28]. The lipids were dissolved in either *n*-decane (30–40 mg/ml) or in squalene (Merck). To modify the lipid composition of membranes, ethanol solution (0.625 mg/ml) of lysophosphatidylcholine (LysoPC, Sigma) was used. In several cases, cholesterol (Calbiochem) was added to a membrane-forming solution in the ratio of 5 lipid to 1 cholesterol (w/w).

Before preparing a membrane-forming solution, azolectin was washed ten times and carefully dried. Chromatographically pure PE and cardiolipin were used without additional purification. Polar contaminations were removed from squalene using aluminium oxide [29].

Formation of bilayers and measurement of their tension. Membranes were formed by the usual technique on a 1–1.5 mm hole in $1 \cdot 10^{-1}$ M KCl solution (unless otherwise specified) at 30°C. To prepare solvent-free bilayers, squalene solutions of PE, cardiolipin and azolectin were used. These bilayers were studied earlier [16,30,31] and found to be stable enough and possess high specific capacity. We were, however, unable to obtain solvent-free phosphatidylcholine bilayers by this method.

Membrane tension σ was measured by the method described by Tien [32].

Membrane interaction. A special cell [31] was used to study membrane interaction. Two bilayers

were pressed one against another due to the difference of hydrostatic pressures in the central and lateral sections of the cell caused by imbedding the calibrated Teflon pivots in the lateral sections. The cell was designed so that a bilayer interaction could be controlled both in directions parallel and perpendicular to the membrane contact plane using binocular microscopes providing 84-fold magnification. In order to standardize the experimental conditions, the difference of hydrostatic pressures was arranged to give contact regions of 0.25–0.35 mm diameter. Ag/AgCl electrodes immersed in a solution were used in the present work, these being connected to Keithley-427 amplifiers and PAR-175 (Princeton Applied Research) generator. The capacity of bilayers was obtained from the amplitudes of rectangular responses to the linearly-swept voltage applied. It was reported earlier [14–16] that recording the amplitude and shape of a capacitive current of two membranes with grounded electrolyte solution allows one to distinguish the main stages of bilayer interaction (FIg. 3). The voltage applied to an electrode in one of the lateral sections of the cell was linearly swept at the speed of 10 V/s with an amplitude of ± 20 mV. The electrolyte solution in the central section was grounded, and the electrode in the second lateral section was used to record the amplitude of capacitive current I_c immediately before the change of the sweep direction. Some time after establishing the plane-parallel contact of membranes (the waiting time of a monolayer fusion, t_{mf}), capacitive current I_c begins to rise. This instant (labelled by an arrow in Fig. 3) corresponds to the initiation of trilaminar structure formation. Further increase of the capacity reflects the increase of the area of a single bilayer in the contact region [16]. This process will be discussed in detail elsewhere. Notice that the shape of the capacitive current changes when passing from the stage of a plane-parallel membrane contact to the stage of a monolayer fusion (cf. Fig. 3). This reflects the termination of the leakage through the grounded electrode in the central section.

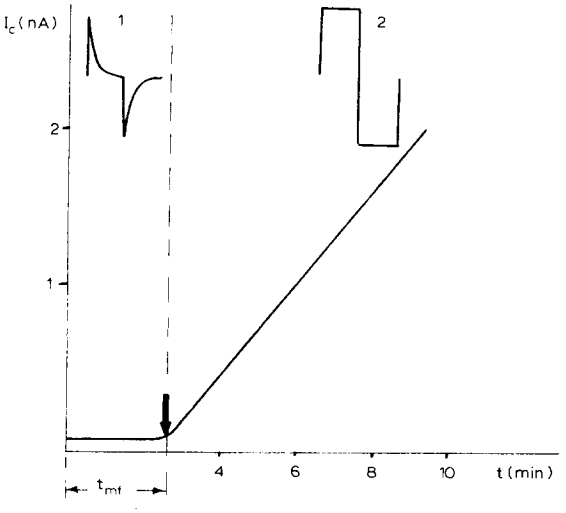

Fig. 3. Recording of a trilaminar structure formation and subsequent growth of the area of a bilayer in a contact region using electrical measurements. Bilayers of azolectin in squalene, 1 M KCl, 30°C. The instant $t = 0$ corresponds to the instant when a plane-parallel contact is reached. The arrow indicates the instant of the initiation of monolayer fusion. The typical current oscillograms for the stages of a plane-parallel contact (curve 1) and monolayer fusion (curve 2) are presented at the top of the figure.

Looking in the direction perpendicular to a contact plane, the results are even more obvious. In this case, an appearance and growth of a black spot can be directly observed in the reflected light against the background of the yellowish region of a plane-parallel contact. The time passing from the instant of a plane-parallel contact to the instant of a trilaminar structure formation (t_{mf}) was measured with the accuracy of ± 1 s. The beginning of a monolayer fusion was registered by the appearance of a minimally visible (under 56-fold magnification) black spot of approx. 10 μm diameter comprising a bilayer region, as revealed by capacity measurements at later stages of a monolayer fusion [16]. Notice that it is practically impossible to observe the formation of bilayer structures of a less diameter, since one has to keep the whole contact region in a visual field simultaneously. As a result, the values of t_{mf} thus obtained appear somewhat overestimated. However, the systematic error seems to be inessential, since the diameter of a visible spot was found to be doubled in less than 3 s at the initial stage of growth.

To control the effective lateral resistance of the intermembrane gap, the characteristic time τ_s of charging two membranes with grounded interspacing electrolyte solution was determined by apply-

ing the voltage swept at 10 V/s with an amplitude of 120 mV [33]. The capacitive current curves recorded (they are similar to curve 1 in Fig. 3) were averaged over 20 single pulses in order to increase the signal/noise ratio and were then used to calculate the characteristic time τ_s.

Linear tension of a membrane edge. In order to obtain this parameter, we have investigated an irreversible breakdown of bilayers [26,34,35]. Mean (averaged over no less than ten measurements) lifetimes, i.e., the time passing from applying the voltage to the current jump corresponding to irreversible membrane rupture [26], were determined for membranes of each composition studied at 4–5 different voltages applied. A membrane rupture was registered using storage oscillography by a voltage jump on 1 kΩ load resistor connected in series with a membrane [26]. The experimental curves were treated in terms of Eqn. 7. Specific capacity C_m and tension σ measured for membranes of a given composition were substituted into the equation. Then, the least-squares method was applied to compute the values of γ and P providing the best agreement between calculated and experimental lifetimes. Notice that the value of P can be used, in principle, to estimate the pore concentration in a membrane [34]. It, however, would require additional model assumptions.

Results

Linear tension of pores in bilayers of different compositions

Experimental points in Fig. 4 represent mean lifetimes for membranes of different compositions at different voltages. The figure displays also theoretical log $t_1(U)$ curves obtained from Eqn. 7 by the least-squares method. At certain values of γ and P, theoretical curves describe sufficiently well the voltage dependences of the lifetimes of membranes. It is noteworthy that since γ^2 enters Eqn. 7 exponentially, even a small change in γ leads to a considerable variation of theoretical log $t_1(U)$ curve. Therefore, this method of determining the linear tension appears quite accurate.

The values of linear tension γ providing best fit of theoretical curves to experimental data are presented in Table I. Depending on a membrane composition, the values obtained are ranged from

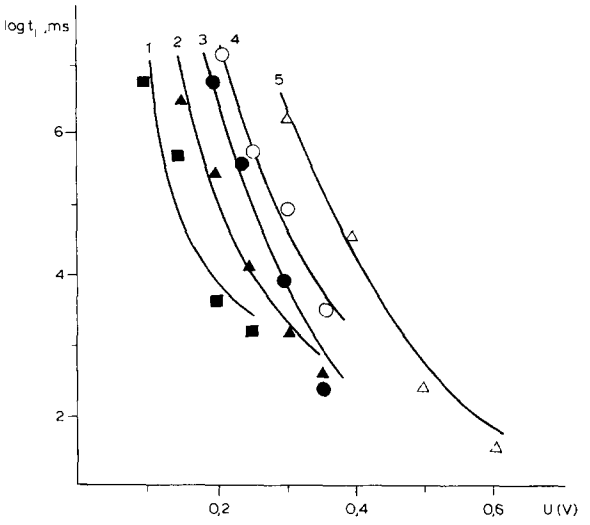

Fig. 4. Voltage dependences of mean lifetimes of bilayers of: (■) PC in decane in the presence of lysoPC ($4 \cdot 10^{-4}$ mg/ml), curve 1, $\gamma = 3.3 \cdot 10^{-12}$ N, $P = 2.5 \cdot 10^{-5}$, (▲) Azolectin in decane, curve 2, $\gamma = 9.2 \cdot 10^{-12}$ N, $P = 1.6 \cdot 10^{-6}$. (●) PC in decane, curve 3, $\gamma = 8.6 \cdot 10^{-12}$ N, $P = 8 \cdot 10^{-8}$. (○) Azolectin in squalene, curve 4, $\gamma = 9.0 \cdot 10^{-12}$ N, $P = 4 \cdot 10^{-6}$, (△) PE in squalene, curve 5, $\gamma = 1.66 \cdot 10^{-11}$ N, $P = 3.1 \cdot 10^{-7}$. Each experimental point (a–e) corresponds to a value averaged over no less than ten measurements ($1 \cdot 10^{-1}$ M KCl). Theoretical curves (1–5) were calculated from Eqn. 7 using the respective values of parameters γ and P.

$0.33 \cdot 10^{-11}$ N (bilayers of PC + $4.0 \cdot 10^{-4}$ mg/ml lysoPC) to $1.66 \cdot 10^{-11}$ N (membranes of PE).

Plotted in Fig. 5 are the values of γ as determined for PE bilayers at different lysoPC concentrations (0; $3.1 \cdot 10^{-4}$ and $4.5 \cdot 10^{-4}$ mg/ml). As seen, modifying the membranes by lysoPC results in decrease of γ.

Monolayer fusion of lipid membranes

The monolayer fusion occurs both in solvent-free and solvent-containing membranes. In both cases, a trilaminar structure formation is an irreversible process. It appears considerably more difficult to separate bilayers without their disruption if a trilaminar structure is already formed than to do it before the monolayer fusion. Visual observations have revealed that even if one succeeds in separating the membranes, they remain connected in a contact bilayer region until a vesicle splits off from one of the membranes. Finally, the vesicle remains attached to another membrane in a contact region.

TABLE I

LINEAR TENSION, γ, CAPACITY C_m AND TENSION σ FOR MEMBRANES OF DIFFERENT COMPOSITIONS

Composition of bilayer	γ(N)($\times 10^{11}$)	C_m (F/m^2)($\times 10^{-3}$)	σ(N/m)($\times 10^3$)
PE/squalene	1.66 ± 0.07	6.6 ± 0.3	2.4 ± 0.2
PE/decane	1.60 ± 0.06	4.4 ± 0.2	2.7 ± 0.3
General lipids/decane	1.04 ± 0.04	3.5 ± 0.2	2.0 ± 0.3
Azolectin/decane	0.92 ± 0.05	3.9 ± 0.2	1.9 ± 0.2
Azolectin/squalene	0.90 ± 0.06	7.8 ± 0.4	2.2 ± 0.2
PC/decane	0.86 ± 0.04	3.2 ± 0.2	1.0 ± 0.3
PE/squalene + lysoPC ($3.1 \cdot 10^{-4}$ mg/ml)	0.77 ± 0.06	6.8 ± 0.3	1.05 ± 0.2
PE/squalene + lysoPC ($4.5 \cdot 10^{-4}$ mg/ml)	0.41 ± 0.05	7.2 ± 0.3	0.33 ± 0.1
PC/decane + lysoPC ($4 \cdot 10^{-4}$ mg/ml)	0.33 ± 0.06	3.5 ± 0.3	0.2 ± 0.1

The visual observations in the direction perpendicular to a contact plane have also shown that, although the monolayer fusion of membranes of any composition inevitably led to the formation of similar structures in a contact region, the presence of a solvent in membranes influenced considerably the process. So, formation of a single bilayer between interacting membranes containing decane proceeds abruptly at a great number of points of a contact region simultaneously. Since, as shown by Berestovsky and Gyulkhandanyan [13], a monolayer fusion of solvent-containing membranes initiates due to the contacts of microlenses attending such membranes, we have focused our attention on studying the interactions of solvent-free bilayers. In this case, quite the reverse, a trilaminar structure formation begins at one or two points (bilayer spots) and then extends slowly over the whole contact region. Therefore, the instant of a trilaminar structure formation against a background of a plane-parallel contact can be determined quite accurately for solvent-free membranes.

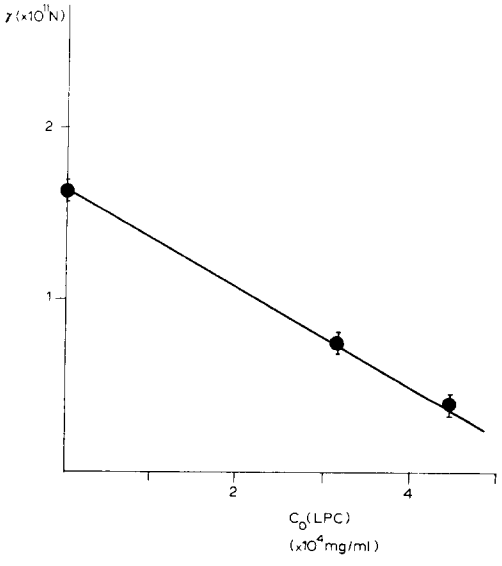

Fig. 5. Linear tension γ of pores in solvent-free membranes in the presence of lysoPC (LPC) in different concentrations. The points shown in the figure were obtained from experimental dependences log $t_1(U)$ (see text for details).

Table II lists the values of mean waiting time of monolayer fusion for solvent-free azolectin, PE and cardiolipin membranes. For the accurate comparison of charged (azolectin and cardiolipin) and neutral (PE) bilayers, the experiments were carried out using 1 M KCl solution to secure efficient screening of membrane charges. In the case of PE bilayers, a monolayer fusion occurred often, even

TABLE II

THE VALUES OF THE WAITING TIME OF A MONOLAYER FUSION, t_{mf}, FOR SOLVENT-FREE MEMBRANES OF DIFFERENT LIPID COMPOSITIONS

Composition of bilayer	t_{mf} (s)
Azolectin	160
Azolectin + cholesterol (5 : 1)	14
Azolectin + lysoPC ($1.4 \cdot 10^{-4}$ mg/ml)	410
Azolectin + lysoPC ($1.4 \cdot 10^{-4}$ mg/ml) + cholesterol (5 : 1)	44
Phosphatidylethanolamine	12 [a]
Cardiolipin	< 1 [a]

[a] The waiting time is measured starting from the instant of the visual rather than real plane-parallel contact (as in all other cases).

before the plane-parallel contact was established which required about 10 s. Therefore, the waiting time of a trilaminar structure formation was measured for these membranes starting from the instant of the visual rather than real plane-parallel contact.

In contrast to other solvent-free membranes considered, the monolayer fusion of cardiolipin bilayers takes place at a great number of points simultaneously just after bringing the membranes in a contact. Therefore, Table II presents only an estimate of $t_{mf} < 1$ s for these membranes.

In some experiments, the composition of bilayers was modified by introducing cholesterol into a membrane-forming solution. Cholesterol decreases considerably the value of t_{mf} (Table II). Unfortunately, real concentration of cholesterol in a bilayer was unknown. Based on the increase of electromechanical stability of membranes and the appearance of a significant conductance current in the presence of nystathin (the data are not presented), it can only be stated that cholesterol was indeed included in bilayers.

Introduction of lysoPC in the central section of the experimental cell influenced considerably the value of t_{mf}. A significant delay of a monolayer fusion was observed in this case. At low lysoPC concentrations (approx. $1 \cdot 10^{-4}$ mg/ml), notable increases in t_{mf} was observed as compared to the control test (cf. Table II). At lysoPC concentrations exceeding $1 \cdot 10^{-3}$ mg/ml, membrane rupture usually 3–4 min after the introduction of lysoPC. Notice that azolectin/cholesterol and PE membranes can endure higher concentrations of lysoPC than azolectin bilayers. The presence of *n*-decane in membranes increases their stability to lysoPC as well. It should be noted that we were unable to obtain a reproducible delay of trilaminar structure formation for bilayers of phospholipids in decane.

Fig. 6 displays the dependence of t_{mf} for solvent-free PE bilayers on the bulk concentration of lysoPC. As seen from the figure, the waiting time increases exponentially with lysoPC concentration. The solid line in the figure was obtained theoretically (see below).

We have also measured the charging time of interacting membranes. For the azolectin bilayer in squalene, τ_s was determined in $1 \cdot 10^{-1}$ M KCl

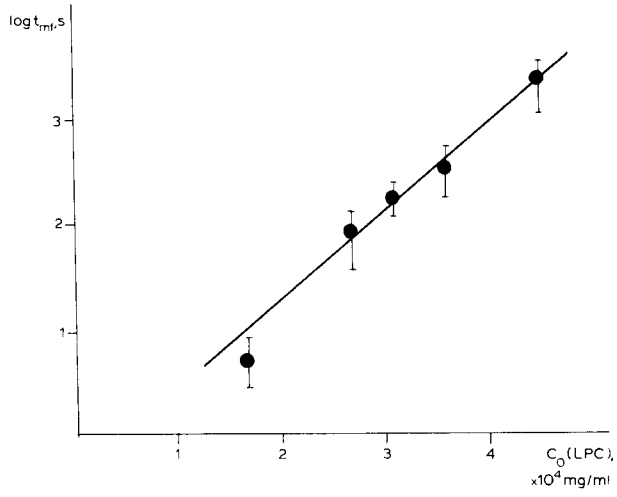

Fig. 6. Dependence of the waiting time t_{mf} of a monolayer fusion of solvent-free PE bilayers on the bulk concentration of lysoPC ($1 \cdot 10^{-1}$ M KCl). The solid line represents the theoretical dependence of t_{mf} on the lysoPC (LPC) concentration.

solution, with the radius of a contact region being fixed at $1.75 \cdot 10^{-2}$ cm. The time obtained was 2.8 ± 0.3 ms. With $7 \cdot 10^{-4}$ mg/ml of lysoPC introduced in the central section of the cell, its value was 3 ± 0.3 ms of that which coincides with the blank test value of τ_s within the limits of experimental errors.

Discussion

Stalk mechanism of a monolayer fusion of lipid membranes

Experimental results obtained in the studies of the monolayer fusion and electrical breakdown of membranes composed of different lipids show that the shape of the lipid molecule is of key importance in monolayer fusion. The values of the waiting time of a trilaminar structure formation between interacting solvent-free membranes were measured (Table II). The waiting times increase in the sequence: cardiolipin, PE, azolectin + cholesterol, azolectin, azolectin + cholesterol + lysoPC. As shown above, the waiting time t_{mf} is less, the less the spontaneous curvature of a membrane monolayer. So, this sequence is in qualitative agreement with the theoretical predictions based on the concept of spontaneous curvature of lipid molecules. Actually, lysoPC possesses posi-

tive spontaneous curvature, whereas cardiolipin, PE and cholesterol are characterized by negative curvatures [18,20]. At the same time, the spontaneous curvature of a monolayer of azolectin, comprising a complex mixture of lipids [36], should have an intermediate value.

The existance of certain qualitative correlation with spontaneous curvatures of membrane monolayers was found, as well, in the investigations of electromechanical stability of bilayers (Table I, Fig. 5). The values of linear tension γ, as obtained from the results of these studies, decrease with the increase of spontaneous curvature. This fact and linear behaviour of dependence of PE bilayers, γ, on the bulk concentration of lysoPC (FIg. 5) is in agreement with theoretical predictions (Eqn. 6).

The most decisive test of the present concepts may be provided by the quantitative comparison of the results obtained using two different experimental approaches. As shown above, the same combination of membrane parameters ξ enters both the expression for the waiting time of a monolayer fusion and the equation for the linear tension of a hydrophilic pore. The value of this parameter was found for PE + lysoPC membranes from the experiments on γ determination. The slope of the dependence $\gamma(c_0)$ (Fig. 5, Eqn. 6) gives $\xi = 6.4 \cdot 10^{-18}$ J/ml per mg. Substituting it in Eqn. 5, we obtain the slope of the theoretical dependence log $t_{mf}(c_0)$. Term B in Eqn. 5 was calculated for $c_0 = 4.5 \cdot 10^{-4}$ mg/ml. Fig. 6 shows that the theoretical dependence thus obtained fits well the experimental points. It is worth noting that no free parameter was used in the present comparison of theory with experiment. Hence, the fact that all experimental points fall on the same straight line, whose slope was predicted by the present theory, proves the validity of this theory.

Thus, both qualitative and quantitative comparison of the experimental data obtained in comparative investigation of irreversible breakdown and monolayer fusion of membranes with the predictions of the above theoretical model demonstrate the validity of the suggested mechanism of a monolayer fusion of lipid bilayers and reveals the key importance of a spontaneous curvature of lipids in this process.

Notice that in treating the experimental data, we have used only the combination of the membrane parameters. However, it seems possible to obtain the values of some individual parameters entering this combination. These are bending modulus D_b and spontaneous curvature ζ of molecules, e.g., PE. The values of these quantities can be obtained from the values of γ for membranes of pure lipids: PC and PE. On the assumption that D_b is independent of a monolayer composition and that the spontaneous curvature of PC equals zero [18,20], it follows from Eqn. 6 and Table I that $D_b \approx 4 \cdot 10^{-21}$ J and $\zeta_{PE} \approx -0.46$/h.

Electrical breakdown and molecular structure of lipids

It is noteworthy that the values of linear tension obtained in this work (Table I) are close to that reported in Ref. [37] as estimated from the radius of pores formed in giant PC liposomes under strong electrical field ($(1.4–2.1) \cdot 10^{-11}$ N). Our method of measuring γ, although less visual than that described by Harbich and Helfrich [37], seems more universal and simple, since it requires neither preparing the giant unilamellar liposomes nor a rather complicated recording system.

An effective value of γ, which can be measured by our method for a bilayer of any composition, characterizes both the effective spontaneous curvature of a membrane (see above) and the ability of a membrane to form hydrophilic pores [38]. It is possible that the increase of the probability of the formation of these pores after a bilayer modification which decreases γ underlies typical changes of electrical properties of membranes observed in some cases (the resistance of a bilayer decreases, the fluctuations and, sometimes, even discrete jumps of its value occur).

It is of interest that equal values of γ do not necessarily imply equal electromechanical stability of membranes of different compositions. Thus, for all potentials studied, the lifetimes of bilayers of azolectin in decane are considerably longer than those of the solvent-free membranes of the same lipid composition formed using squalene solution (Fig. 4; curves 4 and 2). At the same time, the values of linear tension calculated from these curves using the respective values of C_m (0.39 μF/cm^2 and 0.78 μF/cm^2 for decane and squalene bilayers, respectively) and σ ($1.7 \cdot 10^{-3}$ N/m and

$2 \cdot 10^{-3}$ N/m) practivally coincide (Table I). Note that for PE membranes, as well, the presence of solvent only slightly affects the value of γ. This closeness of the values for membranes of the same lipid composition but essentially different mean thickness seems quite explicable. It is known that solvent-containing membranes are non-uniform in thickness [39,40]. The strength of electric field is higher in thinner regions. The field makes these regions still thinner due to the removal of a solvent [40]. It is likely that the pores appear just in these regions where the local membrane thickness approaches the thickness of a bilayer.

The influence of lysoPC on membrane interaction

LysoPC is one of the best studied membrane modifiers. Inclusion of lysoPC in bilayers is known to increase their conductance and to lower considerably membrane tension and stability [32,41]. These effects were also observed in the present work (Table I, the data on the decrease of the resistance of membranes modified with lysoPC are not presented). In addition, the presence of $4.5 \cdot 10^{-4}$ mg/ml of lysoPC in solution increases specific capacity of membranes from an initial value of 0.66 ± 0.02 to 0.72 ± 0.03 μF/cm^2. That is in agreement with the decrease of the thickness of liposomal membranes due to inclusion of lysoPC [42]. The equilibrium constant of fixing lysoPC on erythrocyte membranes and PC liposomes was determined by Elamrani and Blume [43]. It equals about $1 \cdot 10^5$ M^{-1}. If it is accepted that the fixing constant takes the same value in our case, as well, then the simplest estimation for the case where bulk concentration of lysoPC is $5 \cdot 10^{-1}$ mg/ml predicts an approx. 10% content of lysoPC in a membrane. This value seems quite reasonable and is in agreement with the experimental data on erythrocyte hemolysis (lysoPC comprises approx. 10–20% of the total amount of lipids) [44].

Since lysoPC concentrations used in our work are close in order of magnitude to the critical concentration of micelle formation [41], it might be supposed, in principle, that the inhibition of a monolayer fusion by lysoPC is caused by the hindrances in bringing membranes together due to the presence of a considerable amount of micelles in the intermembrane gap. Then, it would be anticipated that addition of lysoPC would lead to a notable change in the effective resistance of the interbilayer gap. However, charging time measurements showed that this is not the case. Thus, the influence of lysoPC on a monolayer membrane fusion is caused by its incorporation in bilayers.

In the experimental system of two interacting lipid bilayers used in the present work, lysoPC did not force complete membrane fusion (i.e., the formation of a membrane tube) even in concentrations close to those rupturing lipid membranes. Moreover, as shown above, modification of membranes with lysoPC delays the monolayer fusion comprising the initial stage of bilayer interaction preceding their fusion. These results agree well with the data obtained for biological membranes. Thus, the fusion of myoblasts and vesicles of myoblast membranes is suppressed by lysoPC in concentrations close to those that we used (approx. $1 \cdot 10^{-4}$ mg/ml), and the increase in lysoPC content in the membrane of Sendai virus decreases considerably the fusogenic activity of the latter [46]. On the other hand, it was reported [47,48] that lysoPC may act as a fusogen. This, however, requires very high lysoPC concentrations (0.1–1 mg/ml) inducing, alongside the fusion, the lysis of cells [47,48].

Thus, to summarize, special experiments on bilayer lipid membranes allowed to ground the following mechanism of a monolayer fusion of lipid membranes. Local bulging defects rise in interacting membrane monolayers. Mutual joining of the defects belonging to different monolayers leads to a stalk formation between the bilayers. Then, the diameter of a stalk increases, which results in a trilaminar structure formation. The stalk energy is determined by the monolayer bending energy, which in turn depends on the effective shape of lipid molecules.

The influence of lipid molecule shape on the process of membrane fusion was frequently discussed in the literature [4,22–25]. The molecules with small polar head and broad hydrocarbon tail (PE, cardiolipin) were demonstrated to facilitate fusion. The electron microscope study of the interaction of liposomes made of such molecules demonstrated that it may lead either to bilayer fusion or to the formation of nonbilayer structures like inverted micelles [49]. The above-mentioned authors suggested that it was the formation of

inverted micelle comprised of substance from interacting bilayers that provoked the fusion process [4]. But it follows from recent investigations that the inverted micelles appear in the system after the fusion and seem to be somewhat stabilized intermediate structures formed in this process [50]. Our paper is devoted in fact to the investigation of such intermediate states which precede the formation of trilaminar structure. Such an intermediate structure visualized in the Fig. 1b might be the apposition of two stalk nuclei. The contact of hydrophobic edges of stalk nuclei with milieu seems energetically to be highly unfavourable. But according to Hoekstra [51], fusion occurs most probably in the region of tight dehydrated contact between membranes. In that case, the energy of interaction between stalk nuclei and milieu can be relatively small.

If it is supposed that fusion is accompanied by the appearance of an inverted micelle, then its nucleus has to be placed between the walls of stalk nucleus (Fig. 1b). In any case, it is the intermediate structure, which condition the energy barrier to be overcome in monolayer fusion and therefore determine the process kinetics investigated in this paper. Our results imply that the incorporation of molecules of positive spontaneous curvature (e.g., lysoPC) into bilayers has the same effect as that which can be calculated from the supposition that the intermediate structure energy is mainly determined by the stalk nuclei energy. We should like to stress that it is right both qualitatively and quantitatively. It means that either the inverted micelles do not arise in this system at all, or their nuclei energy is small comparing to stalk nuclei energy and has no impact on the kinetics of monolayer fusion.

An excess amount of lipid arises in the process of trilaminar structure formation. During the lipid-membrane interaction investigated in this paper, that surplus is removed to the membrane periferee (i.e., to the meniscus). But in the systems without a lipid reservoir (in vesicles and cells), the excess material can be packed into inverted micelles.

We focused our investigation on the primary stage of trilaminar structure formation having in mind that stalk mechanism can operate also during interaction of cell membranes.

Acknowledgements

The authors are greatly indebted to Drs. V.F. Pastushenko, V.A. Ratinov and S.I. Sukharev and to Professor L.M. Chailakhyan for fruitful discussions. The authors are also grateful to Mrs. M.S. Dvoryankina for testing the purity of the lipid species using thin-layer chromatography.

References

1 Poste, G. and Nicolson, G.L. (eds.) (1978) Membrane Fusion, Elsevier North-Holland Biomedical Press, Amsterdam
2 Pinto da Silva, P. and Nogueira, M.L. (1977) J. Cell. Biol. 692, 171–175
3 Portis, A., Newton, C., Pangborn, W. and Papahadjopoulos, D. (1979) Biochemistry 18, 780–790
4 Verkleij, A.J., Van Echteld, C.J.A., Gerritsen, W.J., Cullis, P.R. and De Kruijff, B. (1980) Biochim. Biophys. Acta 600, 620–624
5 Gingell, D. and Ginsberg, L. (1978) in Membrane Fusion (Poste, G. and Nicolson, G.L., eds.), pp. 791–833, Elsevier North-Holland Biomedical Press, Amsterdam
6 Hui, S.W., Stewart, T.P. and Boni, L.T. (1981) Science 212, 921–923
7 Kozlov, M.M. and Markin, V.S. (1983) Biofizika 28, 242–247
9 Borovjagin, V.L., Vergara, J.A. and McIntosh, T.J. (1982) J. Membrane Biol. 69, 199–212
10 Liberman, E.A. and Nenashev, V.A. (1968) Biofizika 13, 193–196
11 Liberman, E.A. and Nenashev, V.A. (1972) Biofizika 17, 1017–1023
12 Badzhinyan, S.A., Berkinblit, M.B., Kovalev, S.A. and Chailakhyan, L.M. (1972) Biofizika 17, 428–432
13 Berestovsky, G.N. and Gyulkhandanyan, M.Z. (1976) Stud. Biophys. 56, 19–20
14 Neher, E. (1974) Biochim. Biophys Acta 373, 327–336
15 Melikyan, G.B., Abidor, I.G., Chernomordik, L.V. and Chailakhyan, L.M. (1983) Biochim. Biophys. Acta 730, 395–398
16 Melikyan, G.B., Chernomordik, L.V., Abidor, I.G., Chailakhyan, L.M. and Chizmadzhev, Yu.A. (1983) Dokl. Akad. Nauk SSSR 269, 1221–1225
17 Helfrich, W. (1973) Z. Naturforsch. 28c, 693–703
18 Israelachvili, J.N., Marcelja, S. and Horn, R.J. (1980) Q. Rev. Biophys. 13, 121–200
19 Markin, V.S. (1981) Biophys. J. 36, 1–19
20 Petrov, A.G. and Derzhanski, A. (1976) J. Phys. Suppl 37, NC3, C3-155–C3-160
21 Israelachvili, J.N., Mitchell, D.J. and Ninham, B.W. (1977) Biochim. Biophys. Acta 470, 185–201
22 De Kruijff, B. and Cullis, P.R. (1980) Biochim. Biophys. Acta 702, 477–490
23 De Kruijff, B. and Cullis, P.R. (1980) Biochim. Biophys. Acta 601, 235–240
24 De Kruijff, B. (1979) Biochim. Biophys. Acta 559, 399–420

25 Madden, T.D. and Cullis, P.R. (1982) Biochim. Biophys. Acta 684, 149–153
26 Abidor, I.G., Arakelyan, V.B., Chernomordik, L.V., Chizmadzhev, Yu.A., Pastushenko, V.F. and Tarasevich M.R. (1979) Bioelectrochem. Bioenerg. 6, 37–52
27 Chernomordik, L.V., Sukharev, S.I., Abidor, I.G. and Chizmadzhev, Yu.A. (1983) Biochim. Biophys. Acta 736, 203–213
28 Kates, M. (1972) Techniques of Lipidology, North-Holland, Amsterdam
29 White, S.H. (1978) Biophys. J. 23, 337–347
30 Chernomordik, L.V., Melikyan, G.B., Dubrovina, N.I., Abidor, I.G. and Chizmadzhev, Yu.A. (1984) Bioelectrochem. Bioenerg. 12, 155–166
31 Melikyan, G.B., Kozlov, M.M., Chernomordik, L.V. and Markin, V.S. (1984) Biochim. Biophys. Acta, 776, 169–175
32 Tien, H.T. (1974) Bilayer Lipid Membranes (BLM), Theory and Practice, Marcel Dekker, New York
33 Pastushenko, V.F., Abidor, I.G., Melikyan, G.B. and Chailakhyan, L.M. (1985) Biol. Membrany, in the press
34 Pastushenko, V.F., Chizmadzhev, Yu.A. and Arakelyan, V.B. (1979) Bioelectrochem. Bioenerg. 6, 53–62
35 Benz, R., Beckers, F. and Zimmermann, U. (1979) J. Membrane Biol. 48, 181–204
36 Darson, A. and Montal, F. (1977) FEBS Lett. 74, 135–137
37 Harbich,, W. and Helfrich, W. (1979) Z. Naturforsch, 34a, 1063–1065
38 Markin, V.S. and Kozlov, M.M. (1985) Biol. Membrany, in the press
39 Henn, F.A. and Thompson, T.E. (1968) J. Mol. Biol. 31, 227–232
40 Benz, R. and Janko, K. (1976) Biochim. Biophys. Acta 455, 721–738
41 Ivkov, V.G. and Berestovsky, G.N. (1981) Dynamical Structure of Lipid Bilayer, Nauka, Moscow
42 Mandersloot, J.G., Reman, F.C., Van Deenen, L.L.M. and De Gier, J. (1975) Biochim. Biophys. Acta 382, 22–26
43 Elamrani, Kh. and Blume, A. (1982) Biochemistry 21, 521–526
44 Weltzien, H.U., Arnold, B. and Reuter, R. (1977) Biochim. Biophys. Acta 466, 411–421
45 Schudt, C. and Pette, D. (1976) Cytobiologie 13, 74–84
46 Poste, G. and Pasternak, C.A. (1978) in Membrane Fusion (Poste, G. and Nicolson, G.L., eds.), pp. 791–833, Elsevier North-Holland Biomedical Press, Amsterdam
47 Poole, A.R., Howell, J.I. and Lucy, J.A. (1970) Nature 227, 810–813
48 Wakanara, M. (1980) Exp. Cell Res. 128, 9–14
49 Hoekstra, D. and Martin, O.C. (1982) Biochemistry 21, 6097–6103
50 Hope, M.J., Walker, D.C. and Cullis, P.R. (1983) Biochem. Biophys. Res. Commun. 110, 15–22
51 Hoekstra, D. (1982) Biochemistry 21, 2833–2840